Bioinspiration & Biomimetics

OPEN ACCESS

RECEIVED
13 December 2021

REVISED
28 March 2022

ACCEPTED FOR PUBLICATION
19 April 2022

PUBLISHED
11 May 2022

PAPER

Sideways crab-walking is faster and more efficient than forward walking for a hexapod robot

Yang Chen, John E Grezmak, Nicole M Graf and Kathryn A Daltorio*

Department of Mechanical and Aerospace Engineering, Case Western Reserve University, Cleveland, United States of America
* Author to whom any correspondence should be addressed.

E-mail: yxc1280@case.edu, jeg100@case.edu, nmg63@case.edu and kathryn.daltorio@case.edu

Keywords: bio-mimetic crab robot, gait optimization, amphibious robots, hexapod robots, legged dynamic modeling, granular media

Abstract

Articulated legs enable the selection of robot gaits, including walking in different directions such as forward or sideways. For longer distances, the best gaits might maximize velocity or minimize the cost of transport (COT). While animals often have morphology suited to walking either forward (like insects) or sideways (like crabs), hexapod robots often default to forward walking. In this paper, we compare forward walking with crab-like sideways walking. To do this, a simple gait design method is introduced for determining forward and sideways gaits with equivalent body heights and step heights. Specifically, the frequency and stride lengths are tuned within reasonable constraints to find gaits that represent a robot's performance potential in terms of speed and energy cost. Experiments are performed in both dynamic simulation in Webots and a laboratory environment with our 18 degree-of-freedom hexapod robot, Sebastian. With the common three joint leg design, the results show that sideways walking is overall better (75% greater walking speed and 40% lower COT). The performance of sideways walking was better on both hard floors and granular media (dry play sand). This supports development of future crab-like walking robots for future applications. In future work, this approach may be used to develop nominal gaits without extensive optimization, and to explore whether the advantages of sideways walking persist for other hexapod designs.

1. Introduction

Legs enable animals [1, 2] and robots [3–26], to navigate particularly challenging terrains. Bio-inspired multi-legged robots [27–29], have shown how using many legs together in a coordinated gait results in fast and stable locomotion. In particular, our group is inspired by crabs which can cross a spectrum of wet to dry sandy terrains and small to large rocks [30, 31].

Many legged robots, inspired by insects, are hexapods that walk forward. Statically stable gaits can be generated with inverse kinematics [32]. Stability margins can be quantified based on center of mass (COM) location relative to the support polygon [33–36].

Contact forces can be used to generate adaptive gaits [37–39]. Dynamic control can achieve desired task accelerations [40]. Bioinspired controllers have demonstrated stable walking through the translation of biological concepts such as central pattern generators [41], genetic algorithms [42], artificial neural networks [43], and spiking neural networks [44, 45]. Forward walking has been demonstrated to be predictable enough for planning [46], simultaneous localization and mapping [47], and walking in confined spaces [48].

Sideways walking has been studied in a relatively smaller number of robots. One important exception in bipeds [49] shows that rotating the hips and knees to operate in the sagittal plane with a non-anthropomorphic gait is akin to walking sideways and reduces roll oscillations [50]. In this design, adding rotation at the hip is best for steering, resulting in a biped leg design that is similar to a crab leg [51]. A robot with four legs that operates this way can switch between quadruped gaits and biped stances [52]. A second important exception is in omni-directional legged gaits [53–55], where robots might use sideways walking to side-step an obstacle or stabilize a lateral perturbation. Others have characterized the stability of sideways walking with dynamic gait stability margins [56] and minimization of foot forces and torques [57].

Robots inspired by crustaceans are especially promising in traversing amphibious terrain. While lobster-like robots with eight legs walk forward in water [26], the crab-like hexapod Ariel walks sideways on land or underwater with invertible legs [3]. Forward bounding gaits have been demonstrated with a swimming quadruped crab-like robot [58]. Sideways walking can be accomplished with compliant reduced-actuated legs in flat and sloped terrain [25]. More recently, Crabster and little Crabster robots have been designed to traverse deep and shallow water, respectively [19, 20, 59, 60]. As amphibious legged robots become more advanced, sideways walking may become more important.

While most engineered robots default to a forward walking gait [17, 18, 30–40, 42–48, 61, 62], most biological crabs default to sideways walking [63, 64]. Furthermore, crab species that develop sideways walking (carcinization) [65] are thought to do so to increase speed [66]. Should crab-like robots walk sideways as well? Or are the mechanics of robots sufficiently different that forward walking is always better? For future robots to traverse the types of terrains that biological crabs excel in, which is better? To our knowledge, direct comparisons between forward and sideways hexapod walking have not been done in robotics and are needed to answer the preceding questions.

In this paper, our goal is to compare forward and sideways walking for a robot that can do both. We propose a simple, direct method for finding a gait that represents the robot's performance potential for a particular walking direction. The robot's workspace first is computed and used to define end effector paths for each leg that utilize their longest feasible stride lengths (SLs) in a particular direction. Then, dynamic simulation is used to iteratively find the minimum leg cycle time for which the paths can be followed with a desired accuracy, resulting in a gait that is both efficient and accurate. This allows us to directly compare velocity and energy usage at different walking heights and SLs for forward and sideways walking, first in simulation, and then on a mobile robot. The simulation platform is Webots [67–69], a widely used and validated robot simulation software [70–76]. The hardware platform is our robot Sebastian [77], figure 1(a), walking on flat ground and in sand. Finally, practical trade-offs of sideways and forward walking are discussed. In future work, this method can be applied to other types of robots to determine appropriate nominal walking gaits and further understand crab-like gaits with robot models.

2. Relationship to other legged gait literature

Analytical research has shown how factors such as velocity, body height, SL, duty factor, joint torque, viscosity, and heat loss can be used to minimize energy cost [78, 79]. For example, smaller duty factors can improve energy cost when speed is increased [80, 81]. However, if the duty factor is too low (<0.5) the robot can become unstable if there are fewer than three legs on the ground at a given time. Thus, in this paper, we assume an alternating tripod gait, common to many other hexapod robots [76, 82–90], which can be generalized to other alternating stance gaits for four or more legs.

Other researchers show that uniformly distributing vertical ground reaction forces results in improved energy efficiency [91]. Even if the ground reaction forces cannot be used in the optimization, minimizing the sum of the squares of joint torques improves the distribution of foot forces and moments [92–95]. Thus, a torque distribution algorithm has been shown to decrease the proportion of heat loss and, as a result, decrease energy cost [96].

It is also possible to use numerical methods to improve gaits over time. For example, using a genetic algorithm [97] to optimize the controller with respect to energetic efficiency, travelled distance and stability of the robot locomotion [98]. More recent robots have shown promise in developing gaits with end-to-end deep learning [44]. A full review can be found in [99]. However, these energy-based strategies can be time consuming, or have uncertainty about achieving a solution, or cannot easily and directly be applied to other articulated legged robots [99].

In the present work, our gait design method is based on the observation that longer SLs often help both speed and energy cost. Detailed animal simulations [80] suggest that to achieve high speed walking with maximum efficiency, longer SLs should be used. Human velocity measured on a treadmill shows that SL changes linearly with velocity outside the transition area [100]. While [80] also suggests there is an optimal stride and swing period for a given velocity, we allow these to vary in our method in order to follow the planned end effector trajectories with a desired accuracy. Thus, our gait design method differs from the existing literature in that while the resulting gaits are not optimized for speed or energy cost, they can be expected to be relatively fast and efficient while following their planned leg trajectories accurately. These modifications allow for their use to compare the robot's performance in different walking directions.

3. Hardware and simulation platforms

We validate our results on our crab-like robot Sebastian, figure 1(a), which has physical parameters listed in table 1. This robot's leg design is loosely inspired by the biological crab species *Pachygrapsus crassipes*, which is a small shore crab that typically walks sideways. Like crabs, the legs end in pointed dactyls [30, 31]. However, while shore crabs are often 5 cm long, our robot is scaled up to 33 cm long to accom-

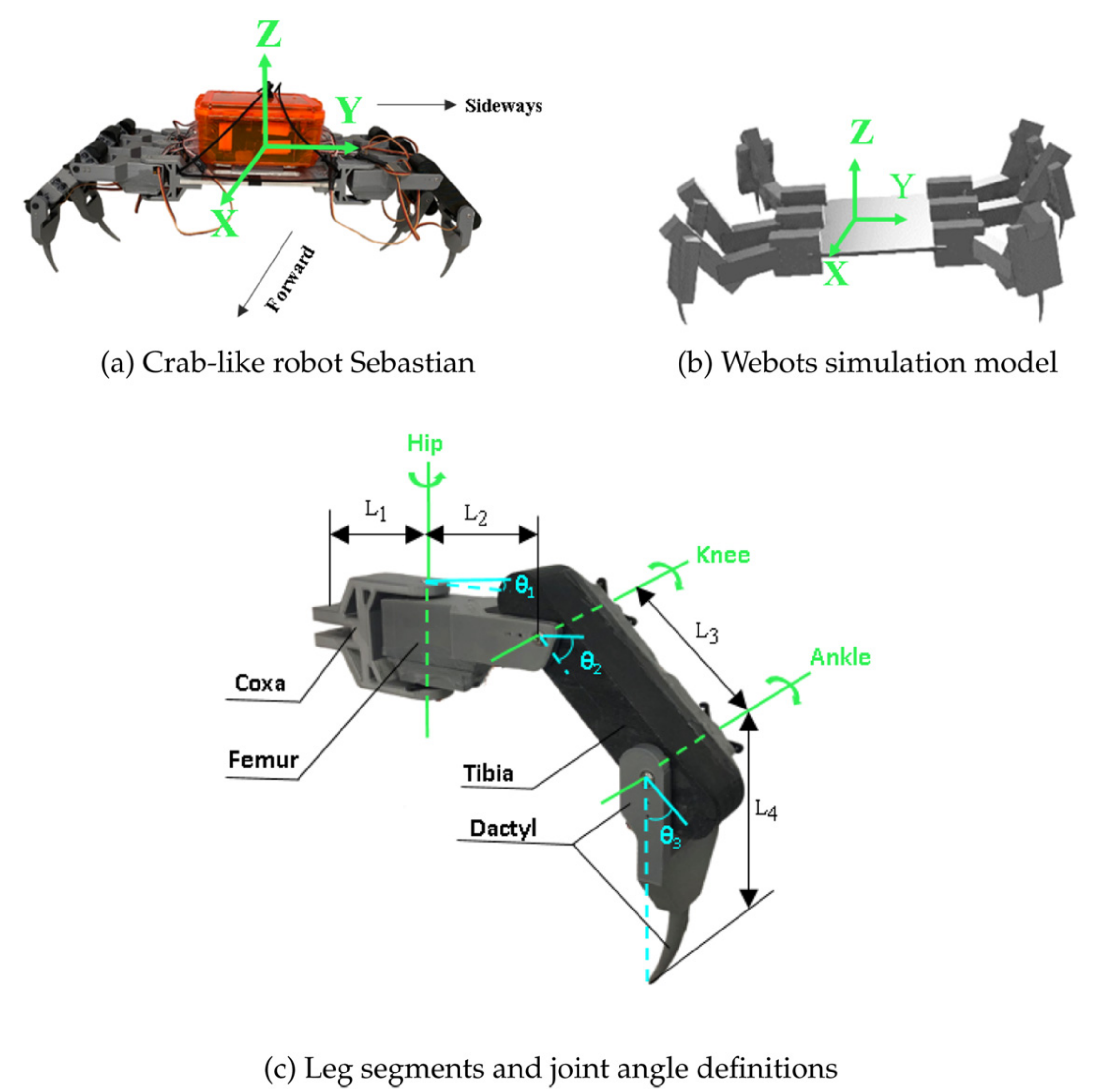

Figure 1. Each of the six legs on our robot (a) and in our simulation (b) have three joints as defined (c).

modate standard SAVOX SV-1270TG motors. Also, the robot is a hexapod in order to have the minimum number of legs for an alternating tripod gait. Thus, there are 18 degree-of-freedom (DOF). All of the leg pieces are 3D printed (MarkerGear M2, PLA, 100% infill). The orange chassis contains batteries and electronics for control and data collection. The robot uses a Raspberry Pi 4B powered by a PiSugar2 Pro as its on-board CPU, which communicates with an 18-pin Pololu Maestro servo controller. A 7.4 V lithium polymer battery powers the motors, and an INA260 power sensor measures the power draw at 25 Hz. The sensor measurements are collected with an Arduino Nano and sent to the on-board CPU.

We use a simplified model in Webots simulation as shown in figure 1(b). Webots is a robotics platform that can model, program and simulate mobile robots with a large number of available sensors and actuators [67–69]. It is used widely in robotics simulation and has been validated in several relevant examples [70–76], with results which are relevant to our study.

Table 1. Robot dimensions.

	Length (cm)	Weight (g)
Total robot	33[a]	3650
Body	20[b]	1800
1 coxa (L_1)	5.4	21.8
1 femur (L_2, 1 servo included)	9.0	95.0
1 tibia (L_3, 2 servos included)	7.5	176.9
1 dactyl (L_4)	12.6	16.6

[a]The minimum length of Sebastian in Y direction (figure 1(a)), when the robot is standing.
[b]The length of Sebastian in X direction (figure 1(a)).

4. Gait design method

Here, the goal of our gait design method is to find fast, stable and low cost of transport (COT) gaits for robots that have articulated legs. Specifically, a common articulation design (e.g. [6–10, 18, 30, 31, 37]) is to have a 'hip' joint that rotates the leg about a vertical axis, followed by 'knee' and 'ankle' joints that have parallel and horizontal axes of rotation, figure 1(c).

Note that human and animal 'hip' joints can rotate in multiple directions, but typical servomotors only rotate in one direction, so this nomenclature is a convenience for this paper. The critical design parameters are the length of the segments between these joints. With such a design a robot can walk at a range of body heights (in Z-direction, figures 1(a) and (b)) and at a range of different step sizes and step heights. A typical forward walk (in X-direction, figures 1(a) and (b)) will involve using broad motions of the hip to move forward and smaller adjustments of the knee and ankle to maintain a straight stride. A sideways walk (in Y direction, figures 1(a) and (b)) will involve greater motions at the knee and ankle to maintain constant height, with only small motions at the hip if steering is required.

To compare forward and sideways gaits, our method, shown in figure 2, maximizes SL and frequency (reciprocal of period (T)) sequentially at a desired height. Subject to our constraints, this should approximately maximize the velocity (v) based on equation (1)

$$v = 2 * \frac{\mathrm{SL}}{T}. \tag{1}$$

*Specifically, when the root-mean-square error (RMSE) between measured and commanded trajectory is $\leqslant 1.2$ cm, swing height error (e_{HS}) is $\leqslant 7\%$, and SL error (e_{SL}) is $\leqslant 9\%$, section 4.3.

Firstly, we calculate the workspace at the desired height and select the longest strides possible within the workspace (either in X direction for forward or in Y direction for sideways walking, figure 3(a)). This is expanded upon in section 4.1.

Secondly, we apply inverse kinematics to find the joint angles for a trajectory with stance that follows full SL and swing that follows a parabolic arc with set height (figures 3(b) and (c) and 4(a) and (b)) in section 4.2.

Thirdly, we simulate in Webots with the planned trajectory and the joint angles with position control in section 4.2, discussed in section 5.

Fourthly, we check if the measured simulated legs in Webots follow the commanded trajectory accurately by tuning the period. We increase the stepping period to decrease the velocity or increase the number of points k (section 4.2) until the robot follows the desired trajectory within a defined threshold of error. This is expanded upon in section 4.3.

Finally, we validate the key results on Sebastian. These results are shown in section 6.

4.1. Finding workspace and stride

Just like biological crabs, our robot's joints have rotational limits, which together with the leg lengths determine the reachable space (workspace) of the dactyl. Joint limits are partly due to interference between the proximal and distal segments if they rotate too far. In addition, servos themselves have rotation limits. Our robot's dactyls intentionally point inward [30, 31] and are therefore not reversible. As shown in figure 4(a), the rotational range for hip joints θ_1 is $(-22.5°, 22.5°)$ and for knee joints θ_2 $(-80°, 20°)$, and for ankle joints θ_3 $(-130°, 0)$. The negative value for θ_1 is the clockwise direction, and the negative values for θ_2 and θ_3 are the downward direction. The 0° for hip joints is shown with bold dark lines in figure 3(b).

We also limit the workspace based on the angle between the ground and the dactyl (AGD) for stable walking, figure 4(a). We consider the AGD to be zero when the dactyl is normal to the ground (vertical). When the dactyl points inward toward the body, the AGD is negative. When the dactyl points outward away from the body, the AGD is positive. The workspace is thus constrained to AGD ranges $(-60°, 60°)$. Larger (positive) AGD results in an excessively sprawled posture and a tendency to slip on flat surfaces. At this AGD range, the robot can successfully extract dactyls at each swing.

In order to have room to walk forward, the middle legs are normal to the body and the front and rear legs are rotated 45° with respect to normal to the body, see figure 3(b). Sideways walking gait uses a configuration where the legs are parallel to each other, as shown in figure 3(c). The workspace in figure 3(a) is determined by forward kinematics with rotational angles' limitations and leg lengths shown in table 1. The height, h, is the distance between the knee rotational axis and the tip of the dactyl. The XY plane shows the workspace with a given height.

Except where indicated, we choose 17.5 cm as the desired height. This height is the minimum for our physical robot testing because of the sprawl limits, sinkage in sand, and the clearance between the body and the ground. With the given height, the workspace of the right front, middle and rear legs for forward walking is shown in figure 3(b) in gray. The left legs workspaces (not shown) are symmetrical with the right legs. Then, we find the full SL for the gait, the red lines in figure 3(b). Based on geometry, figure A1 in appendix A, the full SL for the right front, middle and rear legs are the same. Figure 3(c) is the workspace for sideways walking, as legs are parallel and the hip joints are not used. The full SL is 15 cm. The gray shape shows the available workspace. The blue (green) displays the full stride (half stride) for sideways walking. Note that the half stride experiments are performed with the distal part of the workspace, because it is more stable.

4.2. Trajectory inverse kinematics

In both forward walking and sideways walking, the stance phase trajectory is a straight line and the swing phase trajectory is a parabola with 6 cm swing height,

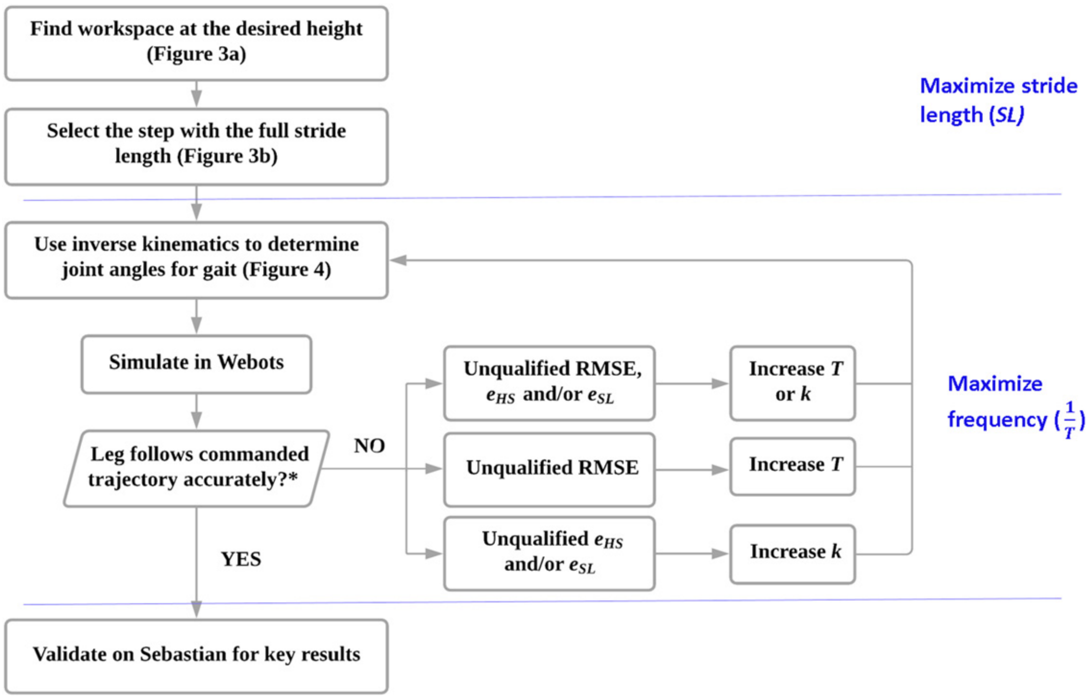

Figure 2. The process for determining gaits for forward and sideways walking.

as in figure 4. We choose 6 cm as the swing height, because this is sufficient for extracting dactyls from the sand. A higher swing will be able to step over larger obstacles, but will cost more energy during the swing phase and may slow the required stepping frequency. A RMSE analysis of the simulated end effector trajectory, found that 66% of the trajectory error for forward walking occurs in the swing phase. Consequently, we expect an increase in the swing height to result in a decrease in speed. Similarly, about 55% of the trajectory error sideways walking is in the swing phase, so we expect increasing the swing height to decrease speed. Figure 4(a) is the trajectory for the right middle leg for forward walking and figure 4(b) is the trajectory for the right legs' sideways walking.

First, we use inverse kinematics to determine joint angles required for points along the path. Then, we use polynomial fitting to generate the trajectory for Webots simulation (with convergence criteria of $R^2 \geqslant 90\%$).

In stance, the trajectory, figure 4, is defined by endpoints A and B, which are determined by the full stride in figures 3(b) and (c). We divide the stride into k equal segments of equal time. At each of the resulting $k+1$ points, we use inverse kinematics to find the joint angles, then use polynomial interpolation to determine the desired joint angles (θ_1, θ_2, and θ_3) as a function of time for position control. We start with $k = 9$, and increase it as described in section 4.3 and figure 2.

In forward walking swing phase, the hip angle (θ_1) increases at a constant rate and we use inverse kinematics to determine the knee and ankle angles (θ_2 and θ_3) that keep the end effector on the desired parabolic trajectory, figure 4. Thus the $k+1$ points are determined by increments of $(\theta_{1B} - \theta_{1A})/k$, where θ_{1B} and θ_{1A} are the θ_1 for point B and A respectively, figure 4. In sideways walking swing phase, the x direction speed is held constant and thus the $k+1$ points are determined by increments of $(x_B - x_A)/k$, where x_B and x_A are the x positions for points B and A respectively, figure 4.

4.3. Period tuning

After determining the trajectory with inverse kinematics, we determine the fastest possible frequency for an accurate step. In order to compare forward and sideways walking with equivalent metrics, we set a threshold for the end effector trajectory accuracy. Specifically, we chose 8% of the full SL, which is 6% of Sebastian's body length, and 4% of Sebastian's leg length. When the robot cannot keep up with the desired trajectory within the threshold, the speed is too fast. In addition, we choose the criteria for margin of error of swing height (Δ Hs $\leqslant 7\%$) and SL (Δ SL $\leqslant 9\%$). Except where indicated, the periods used for all the gaits in this paper are based on this method.

Periods are evaluated iteratively in Webots simulations. For each period, the x, y, and z coordinates of the end effector are measured and compared with the commanded trajectory, with 33.3 Hz as the sampling frequency. If the RMSE is less than 1.2 cm, the

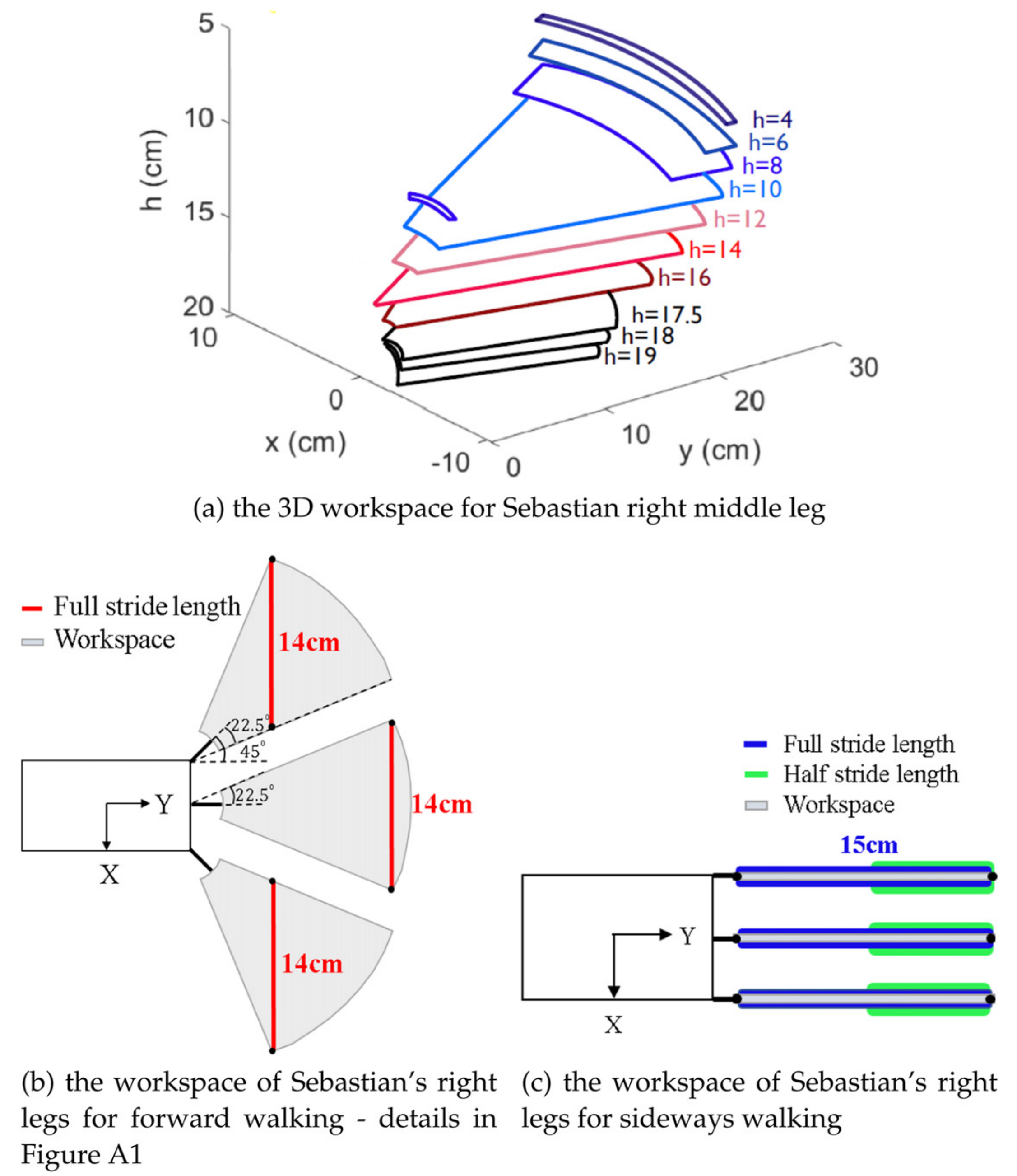

Figure 3. The workspace of the dactyl tip (a) determines the available SL for walking (b) forward or (c) sideways. The black lines in (a) represent the height chosen to figure out the effect of height. Note that for comparison, we consider a half-stride sideways walk (green) in (c) that uses only the distal part of the workspace (gray) because that results in more stable walk.

speed is increased. If RMSE, e_{SL} and/or e_{HS} thresholds are exceeded, the period T or the number of points k is increased; if RMSE exceeds 1.2 cm, the period T is increased; and if e_{SL} and/or e_{HS} exceeds the defined thresholds, k is increased, according to figure 2. The resulting period is used for the simulation and validation gaits.

This process is demonstrated numerically in table 2. Here we show that for forward walking we can use a smaller period, decreasing until the normalized RMSE (the RMSE divided by the threshold) exceeds 100%. Thus, the period we selected was 1.44 seconds. Similarly for sideways walking, the periods are longer (and the SLs are also longer).

Note that the period resolution (0.18 seconds in table 2) is sufficiently small since the maximum velocity error from the period resolution ($<$0.03 m s^{-1}) is smaller than the difference between the maximum velocities (0.085 m s^{-1}) for sideways and forward walking. Furthermore, since we can analytically predict the velocity using equation (1), we can further show that the theoretical error would be less than the reported differences between maximum sideways and forward velocities.

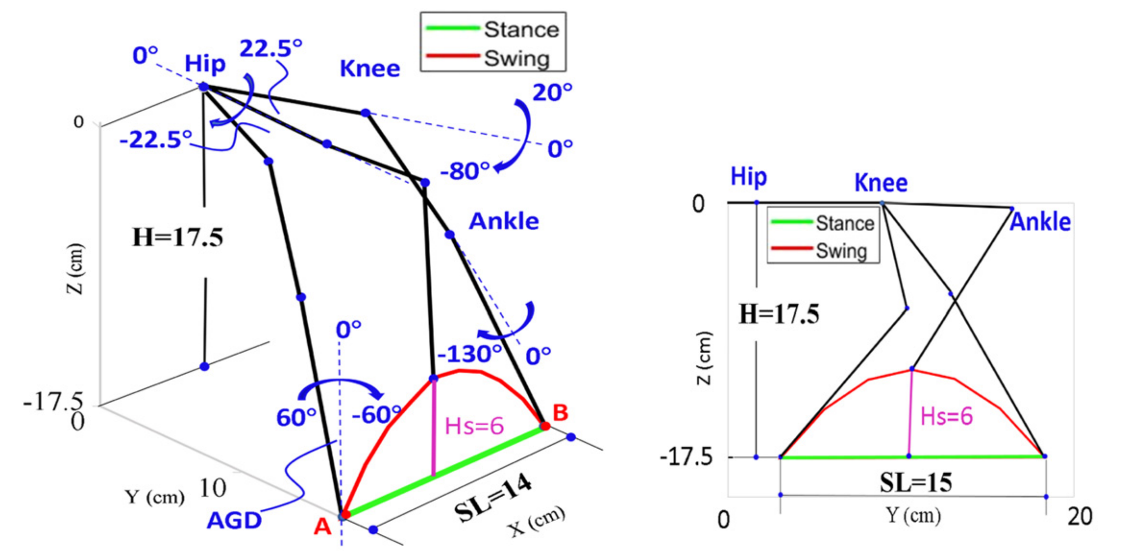

(a) Middle leg trajectory (forward walking) (b) Leg trajectory (sideways walking)

Figure 4. In both forward (a) and sideways (b) walking, the stance trajectory is a straight line (green) and the swing trajectory is a parabola with height $Hs = 6$ cm.

Table 2. RMSE between measured simulated trajectory and commanded trajectory and simulation velocity with different periods for full stride forward and sideways walking—the stride for forward walking is 14 cm and sideways walking 15 cm. *T* is the period. The bold data is the proper periods we choose.

	Period *T* (s)	1.8	1.62	**1.44**	1.26	1.08
	Normalized RMSE	102%	96%	**90%**	105%	113%
Forward walking	Velocity (m s^{-1})	0.109	0.105	**0.116**	0.134	0.153
	period *T* (s)	2.4	1.86	1.68	**1.5**	1.32
	Normalized RMSE	91%	94%	95%	**88%**	100%
Sideways walking	Velocity (m s^{-1})	0.132	0.166	0.186	**0.200**	0.227

5. Simulation preliminary results

The gaits used in both forward and sideways walking are tripod gaits. In Webots, the robot is walking on a linoleum floor where the friction coefficient is 0.5. The velocity is measured from total position, *d*, moved after ten full steps, and excludes the steps before the first 0.3 seconds, to eliminate acceleration transients. The position is obtained from the GPS node in Webots. Energy consumption, *E*, is measured by the battery node. COT is calculated based on equation (2)

$$\mathrm{COT} = \frac{E}{mgd} \tag{2}$$

where *g* is the acceleration of gravity and *m* is the mass of the robot.

5.1. Effect of stride length

Our Webots simulation confirms that using the longest SL results in the fastest and the most efficient gaits, figure 5. At the chosen height of 17.5 cm, we compared behavior with shorter strides. In sideways walking, with a full SL of 15 cm, we consider the most distal portions of the SL to take shorter strides. In forward walking, with a full SL of 14 cm, the middle leg strides are centered while the front and rear legs are spaced as far as possible from the middle leg (forward and rear parts of the full SL). Decreasing SL monotonically decreases velocity and increases COT until steps are smaller than the step height. At these small SLs, the robot is even slower and less efficient.

Furthermore, it is clear that sideways walking is almost twice as good, both in speed and efficiency for a given SL. Thus, a sideways walk with a half stride (7.5 cm) should be more efficient than a forward walk with a full 14 cm stride. This hypothesis is validated on the hardware in section 6.

5.2. Effect of body height

Next, we consider whether the superior performance of sideways walking is unique to the height we have chosen. To do this, we consider two slices of the full 3D workspace at the bottom of figure 3(a) for $h = 18$ and 19 cm, respectively, and find their maximum SL. In order to do so, for sideways walking, we consider a *ZY* plane through the center of the workspace in figure 3(a). For forward walking, we consider a *XZ* plane through the widest part of the

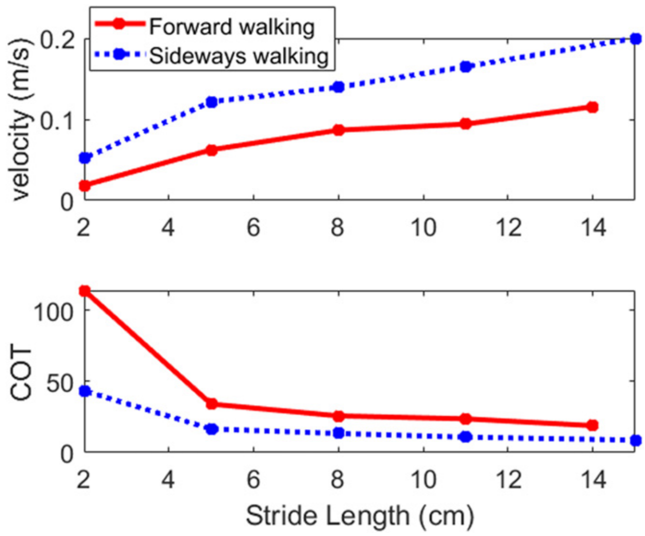

Figure 5. In simulation, the maximum stride yields the fastest and most efficient gait. The sideways walking is twice as good as the forward walking given the same stride. And the half stride (7.5 cm) sideways walking is better than 14 cm full stride forward walking. This is validated with hardware in section 6.

workspace in figure 3(a). In the same way, the stride planes for different heights, figures 6(a) and (b), the maximum SL at each height can be observed, and is plotted in figure 6(c). Note that when height is greater than 10 cm, front and rear legs have the same maximum SL as the middle leg's, as shown with the isosceles triangle in figure A1. However, when the height is less than 10 cm, the full stride limits are different for middle and front/rear legs.

For both forward walking and sideways walking, a step that holds the body at a constant height of less 10 cm will be limited in size based on the joint angle limits (see how the workspace plot tapers at the top of figures 6(a) and (b)). Limiting factors include the rotational joints and AGD limits, and the front and rear legs rotating 45° with respect to normal to the body. In particular, for sideways walking, the workspace of is non-contiguous if the height is below 10 cm, suggesting that the robot could take small steps with large y position (>20 cm, highly sprawled) or small steps with $y < 15$ cm, but would not be able to move between these regions within a single stance. This suggests a lower limit on walking height based on joint angle limits.

For walking with body height above 10 cm, the available SLs are different for forward walking and sideways walking. For forward walking, figure 6(b), there is a maximum SL near 10 cm, and a gradual decrease at higher heights. For sideways walking, the maximum SL is at closer to 14 cm height, with a steeper decrease at higher body heights.

We can only validate kinematic predictions for the upper range of body heights, due to limitations of highly sprawled postures for our physical robot in sand, and we focus our simulation in this range. Since the height is the measured from the center of the hip joint, when the height is too low the chassis drags along the ground. This is exacerbated when the dactyls penetrate the sand. The gray bar in figure 6(c) shows the appropriate height ranges for our robot experimentally. Fortunately, that range includes a critical intersection at which forward walking SLs exceed SLs of sideways walking. Thus, we tested this limited height range at three points (17.5 cm when the sideways SLs are longer, 19 cm when the forward walking SLs are longer, and 18 cm when they are approximately equal). This represents the upper height range possible since at 20 cm, the workspace tapers to zero.

For all three of the heights examined, sideways walking is faster, and energetically superior. The differences become smaller when the height is larger, and sideways walking worsens. Specifically, the speed of the sideways walking robot is 73% faster at the lowest height and 40% faster at the highest height. The COT of the forward walking robot is 127% higher at the lowest height and only 56% higher at the highest height.

Overall, the best walking is expected to be sideways walking at the lowest possible body height, 17.5 cm. Perhaps in future hardware designs, legs could be mounted below chassis and sand penetration could be limited with dactyl design to enable even more sprawled posture comparisons at heights close to 14 cm. However, heights below 10 cm would not be desirable with current joint and angle limits.

6. Results

We compared three gaits: the full stride gaits for sideways and forward walking (the best possible gaits), and a half stride sideways gait, figures 3(b) and (c). This half stride gait should be comparable to the forward gait at full stride since our prediction was that

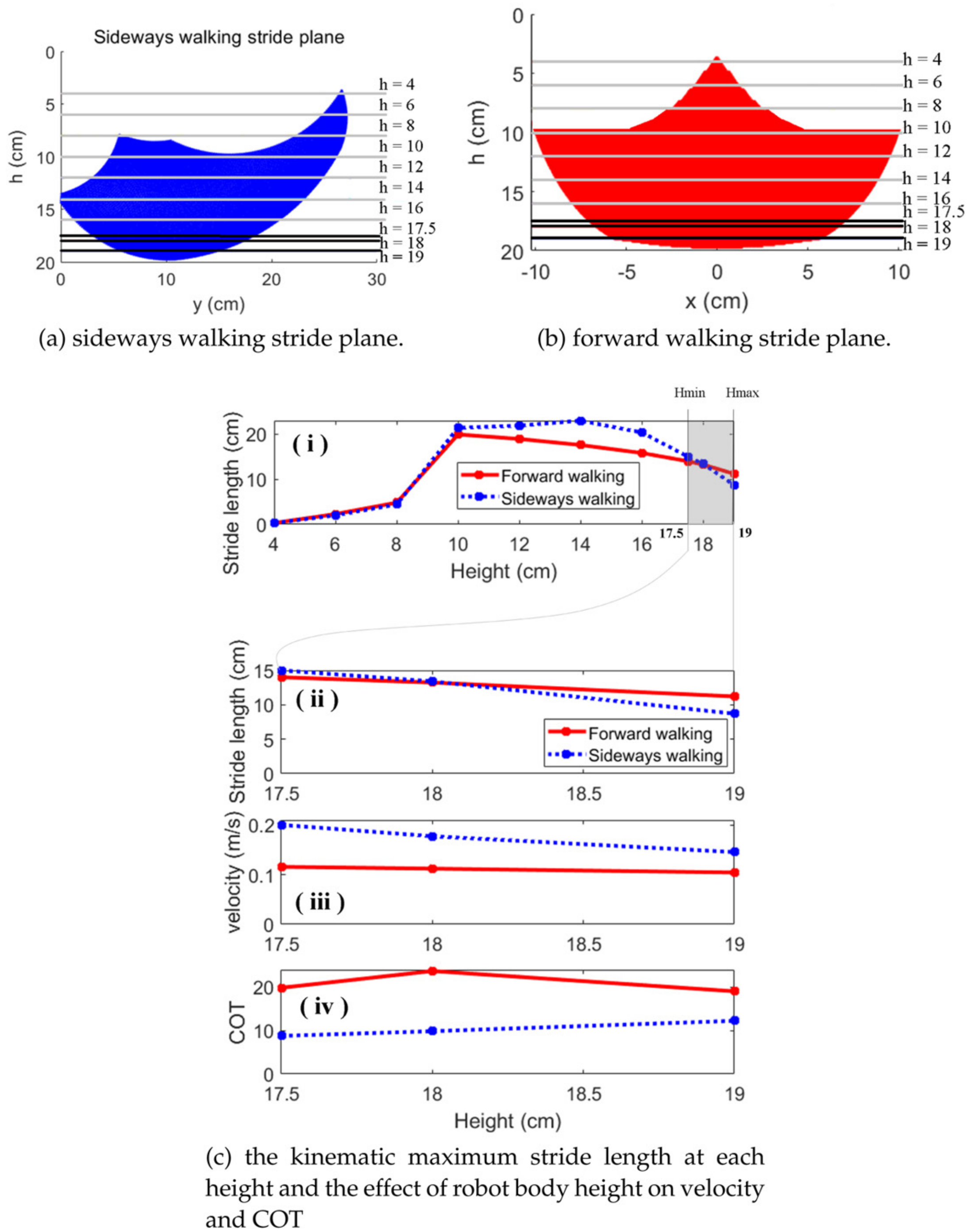

Figure 6. For forward (a) and sideways (b) walking, the legs operate in a plane of the workspace, the stride plane. Thus, the full SL varies with the walking body height, H (c). The gray area in (i) shows the region of feasible heights for our hardware prototype, which are between H_{min} and H_{max}. Expanding to examine the feasible range, (ii) shows that when the height is larger than 18 cm, the full SL for forward walking is bigger than sideways walking. (iii) Shows that the simulation predicts higher velocity when sideways walking throughout this range of heights with the full SL. (iv) Shows that the COT is also better (lower) for sideways walking than forward walking for this range of heights. The h values in (a) and (b) are the same as figure 3(a), and heights marked with black lines: 17.5, 18 and 19 cm are used for (c), (ii)–(iv).

the sideways gait was roughly twice as good. In addition, such a gait with shorter-than-maximum steps could be a valuable baseline for realtime SL adaptation in the presence of obstacles [18]. The period for half SL sideways gait is 1.2 seconds, as opposed to the period for full sideways gait of 1.5 seconds (table 2) and is determined in the same method.

Sideways and forward walking are compared in four progressively more realistic evaluations from kinematic prediction, to simulation, to walking on

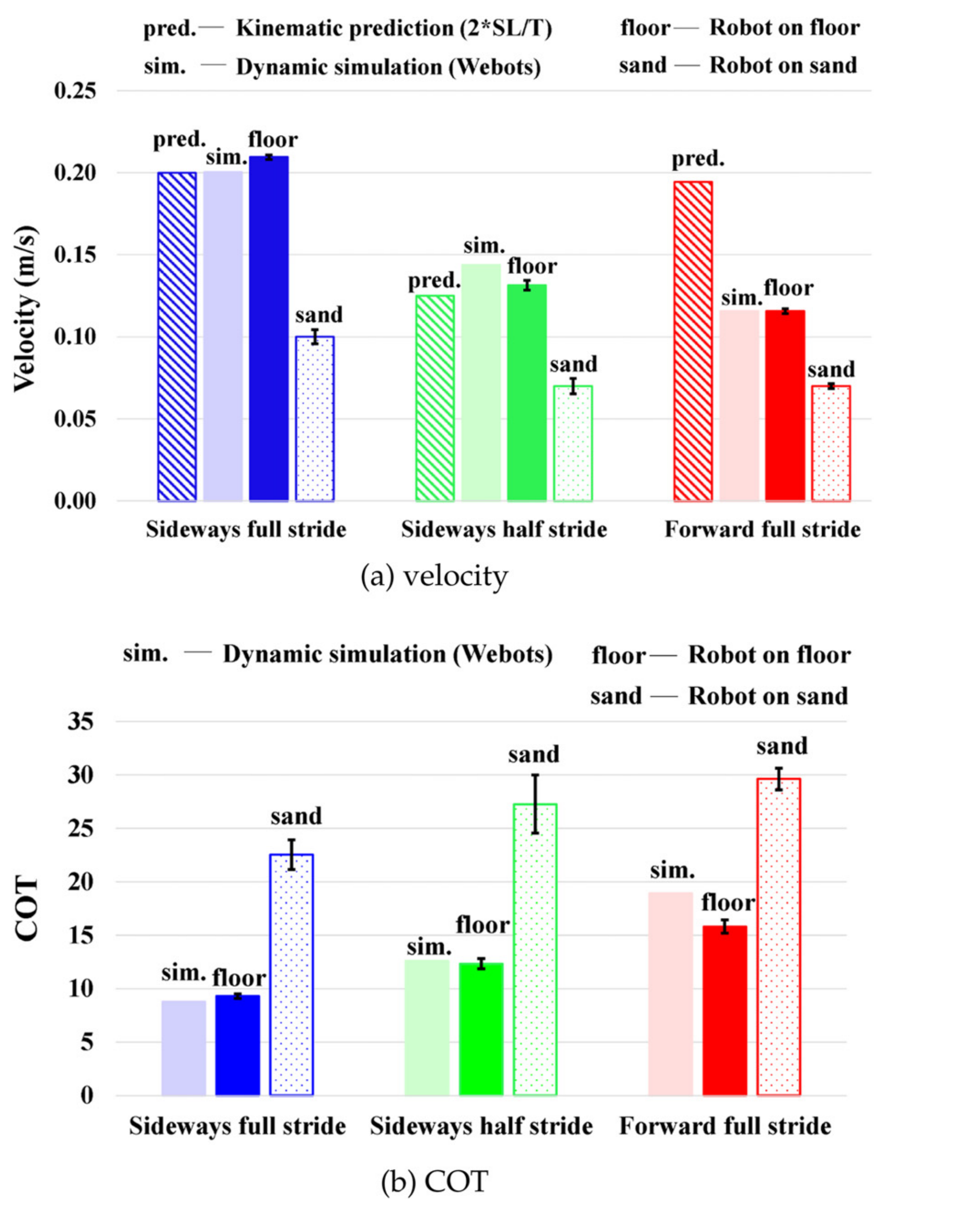

Figure 7. When comparing kinematics, Webots, and physical robot performance on smooth ground, velocity agrees well (a). Energy costs can be compared as well (b). Even though sideways walking is better on robot than predicted in simulation, sideways is more energy efficient with lower COT. The height of the bars means the average velocity (a) and COT (b) over ten trials tests. The error bars show the standard deviation (STD) of velocity and COT.

hard floors, to walking in dry sand, which represents one of the more challenging terrains for crab-like robots.

First, the kinematic prediction of velocity is calculated using equation (1), with the SL and period determined as above. As is clear from figure 7(a), the kinematic predictions of the speed for forward and sideways walking are similar. Thus, dynamics are needed to understand the differences.

Secondly, based on the dynamic simulation results in Webots, figure 7(a), when the interaction with a smooth low-friction ground is included, forward walking is much slower than sideways walking and slower than the kinematic prediction, as shown in the previous section. A contributing factor is the degree of slip between the dactyl and the ground. Specifically, while the middle legs tend to have small slip, the front and rear legs for forward walking have a high amount of backward slip, which we diagram in figure 8. In sideways walking, middle legs slip slightly more than front and back legs, since it is opposed by two legs, however the degree of slip is less. Additionally, forward walking involves more lateral motion of the body, which does not occur in sideways walking.

The average velocity for the full stride sideways walking is 62% larger than the half stride sideways gait, which validates that the full SL gait yields the

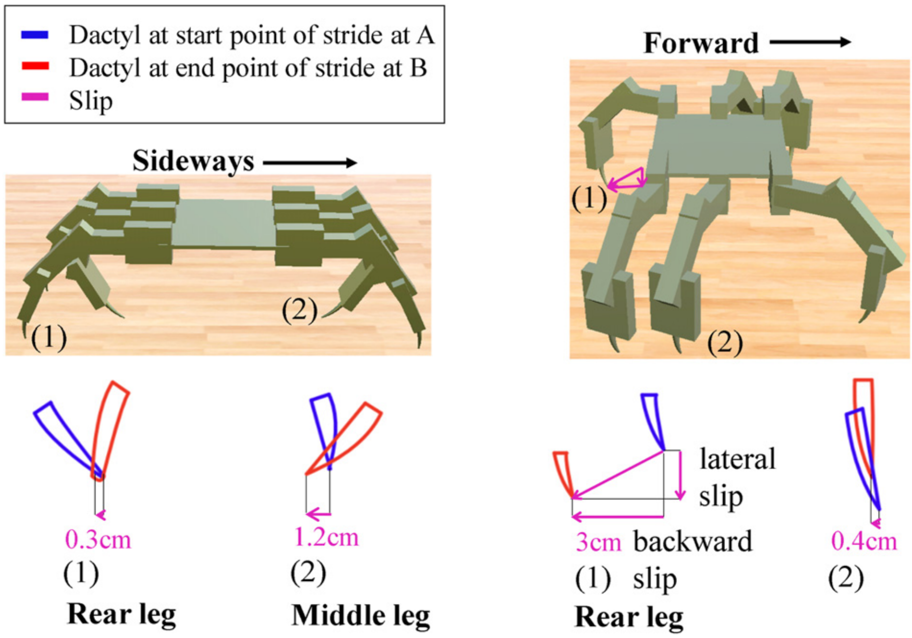

Figure 8. The dactyl angles at beginning and end of stride show small slippage of all legs for full stride sideways walking (a) and small slippage of middle leg and big slippage of front and rear legs for full stride forward walking (b). The magenta arrows show the slip direction. The magenta numbers show the slip value. Note that points A and B are shown figure 4.

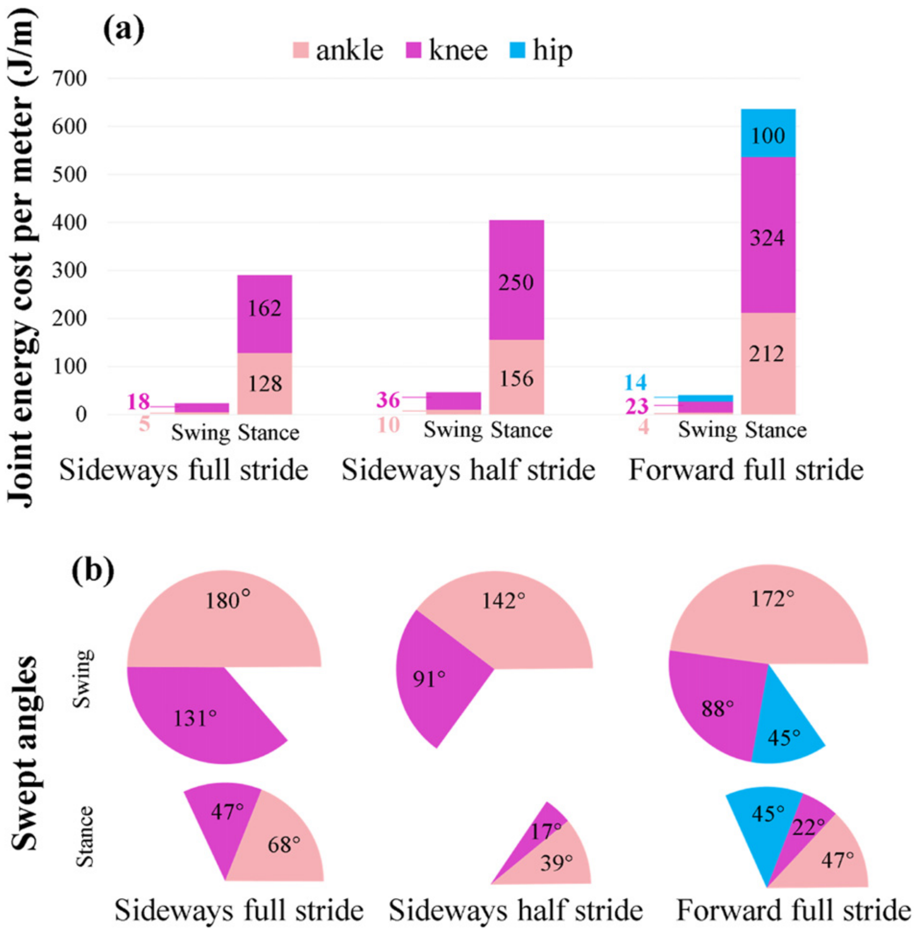

Figure 9. The joint energy cost per meter (a) and swept angles (b) were measured for each joint in the simulated Webots gaits.

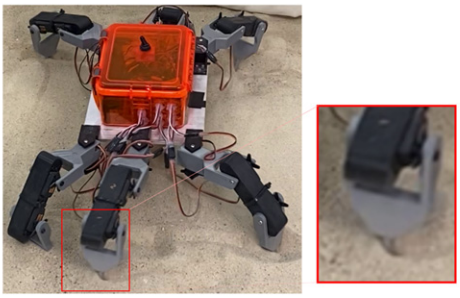

(a) Sebastian walking forward in sand.

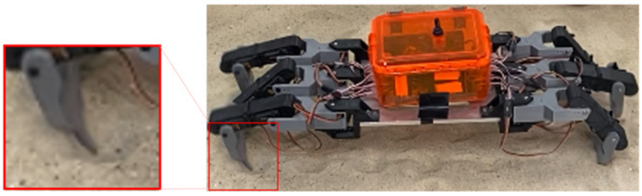

(b) Sebastian walking sideways in sand.

Figure 10. With the forward walking gait (a), the dactyl tends to pull out of the sand. While for sideways walking (b), the dactyl tends to roll on the sand, as shown in inset details. The total depth of sand is 7.5 cm.

optimal gait. Note that low-friction environment was chosen because it simplifies modeling (especially compared to granular media), and can be directly compared with walking on the lab floor (i.e. the solid bars in figure 7(a) are similar to the shaded bars).

Thirdly, we validate these simulation results with physical hardware, our robot Sebastian. For each gait, we did ten trials of ten strides each on the linoleum floor and kept all parameters the same as the simulation.

The hardware trials validate the velocity predictions from Webots. Specifically, the Webots predictions are 95% accurate. The slight difference may caused by the error from the fabrication, servos' motion, power sensor and parts connection of Sebastian. This supports our conclusion that the fastest sideways walking gait is *1.05 body lengths per second, 75% faster than the fastest forward walking gait, figure 7(a).

Although the forward walking COT is in the range reported by other hexapod robots, e.g. [101], walking sideways lowers COT by 40%, as shown in figure 7. One possibility was that the lower COT is due to the fact that sideways walking only uses two joints per leg (ankle and knee) whereas forward walking uses three (ankle, knee and hip). To investigate whether this is the case, we separated the energy contribution of each joint for each gait, figure 9(a). This calculation is from ten full strides of the simulation joint torques, which is expected to be similar to hardware due to the overall similarity of COT in figure 7. As expected, the energy used by swinging legs is less than the energy used by stance legs (since leg mass is small relative to body mass). However, one potentially surprising result is that even without the energy used by the hip joint, sideways walking is still more efficient, since the knee and ankle require more energy for forward walking. This is true despite the fact that the knee and ankle move more than (full stride) or comparable to (half stride) forward walking, figure 9(b).

Thus, we conclude that in addition to the number of joints utilized, the higher COT is due to energy lost from slip, figure 8 and other dynamic effects, including rotation of the body, figure C1.

Finally, we tested the robot on dry sand, figure 10, since granular media is a natural substrate for crab-like locomotion. The sand is Pavestone natural play sand. The robot walked in ten directions in the sand tank to minimize any error caused by differences in the sand surface. For each gait, we did ten trials in sand and kept all parameters the same. Every trial includes ten full strides.

For all gaits, sand slows down the robot, which is consistent with other papers [30, 31]. The COT is also increased, as expected, because of the resistance of the sand, increased slip, and more variable and unstable steps. Forward gait velocity performance reduction percentages are lower than sideways walking, because the sand reduces the slippage on the front and rear legs when compared with the linoleum tests in appendix B.

Nonetheless, the full stride sideways gait is both faster and more energy efficient than the full stride forward gait in sand. A half stride sideways gait is comparable to the full stride forward gait in efficiency and speed.

7. Conclusions

Taken together, our results suggest sideways walking at the lowest height, utilizing the full range of motion is best for energy efficiency and speed.

By both metrics, sideways walking appears better than forward walking. Sideways is more efficient and faster at all heights in the range of our robot. Sideways is better on flat smooth terrain and on dry granular media. Sideways gives better speed per SL. Sideways gives longer SLs at low heights. The single exception seems to be that forward walking enables longer SLs when the robot is at its maximum height but not enough to translate into faster or more efficient walking.

In addition, we demonstrate a gait design method that is effective in variable terrains. On tile floor, sideways walking is comparable to kinematic and simulation predictions. On sand, as expected, all the robot gaits are slower and less efficient. However, the relative speeds and efficiency on sand follow the same patterns. This suggests that the gait design method is sufficiently generalizable to varying terrain. Since beaches are of particular interest for crab robots, testing on rocky and wet substrates will be interesting for future work. However, our prior work [30, 31] suggests that compact wet sand may be easier to traverse than dry sand since wet sand is strengthened by capillary forces, and the increase in shear strength can reduce leg slip. Thus, our experiments here are meant to convey the best and worst case for walking on beaches, showing sideways walking is superior in both.

This work reflects the differences in a common leg design configuration for forward walking robots [76, 82–86, 89, 90]. The fact that it is common for forward walking makes it all the more surprising that sideways walking is more efficient and reflects an opportunity to use these already designed robots differently.

8. Discussion

8.1. Comparison with biology

Biological crabs are diverse and able to traverse a wide range of terrains [102]. As is visible from table 3, some species are larger, and some are smaller than our hexapod robot. Inhabiting a range of ecological niches, they also display a wide range of walking speeds, both above and below the speed of our robot when normalized by leg length [103–105, 105–108]. The crabs closest in size to our robot are king crabs, like *Paralomis formosa* [103–105] and Kamchatka crabs [105, 106]. Since the reported studies are ecological rather than biomechanical, some of the walking recorded could include sideways walking. However, like all king crabs, their joint anatomy enables forward walking rather than the sideways walking characteristic of true crabs of order *Brachyura* [105]. The king crabs have a speed to leg length ratio of around 3, which is similar to our robot's forward walking speed to leg length ratio of 4. Meanwhile, examples of *Brachyura* crabs are much faster, in the case of the ghost crabs, reflecting fast muscle actions and dynamic gaits in which the step length is extended by jumping through the air [109]. As walking robots improve to serve in tedious and hazardous tasks, bio-inspiration from crabs can provide important insights.

Our robot's preference for sideways walking is consistent with evolutionary biology [66]. In multiple instances forward walking animals have developed sideways-walking crab-like anatomy in a process called carcinization [65]. Sideways walking is thought to help the animal walk faster, but may reduce the pleon and claw size [65].

8.2. Fundamental trade-offs for sideways and forward walking

Our robotic experiments suggest that a preference for sideways walking may be due to mechanical differences in sideways and forward walking that are shared between robots and animals. There are several key differences in walking directions fundamental to both robots and animals.

First, forward walking uses three joints per leg, while sideways walking only relies on two, since the hip angle can be constant during sideways walking. Using the hip joint for forward walking contributes to the energy cost (15%, figure 9) but does not result in an increase overall speed. This is not to say that hip joints are not valuable. The tests in this paper use a fixed gait, but animals and robots in challenging terrain can use a hip joint in footfall planning and maneuvering in both forward and sideways walking. Therefore, there are advantages to having DOF available that are not used in nominal walking, and future study could investigate this further.

Second, sideways walking enables qualitatively different use of the dactyls. Sideways walking keeps dactyls in a plane, while forward motion rotates dactyl. This is pictured in figures 8 and 10. While in both cases the AGD limits are the same, in sideways walking the dactyls can rotate to follow the curve of the dactyls, almost rolling like a wheel over the terrain, which can be seen in appendix B and figure 10. For the three legs in the front, this motion may help slide over terrain. For the three legs in the rear, this might help compact the granular media before push off. In contrast, in forward walking, the dactyls rotate sideways during stance, digging the tips out as the AGD increases, figure 10 and appendix B. Loosening the terrain around the dactyl may make it harder to anchor to the ground in surf zones. There may also be trade-offs for probing the substrate or burrowing in granular media.

Thirdly, forward walking induces more body rotation and dactyl slip. While the slip at the middle legs,

Table 3. Normalized velocity for Sebastian robot and several crab species.

Species	Mass (kg)	Leg length (cm)	$\frac{\text{velocity}}{\text{leg length}}\left(\frac{\text{mm/s}}{\text{cm}}\right)$	Preferred walking direction	References
Pachygrapsus crassipes	0.02	5	17[a]	Sideways	[110–112]
Ghost crab	0.05	9	178	Sideways	[113–115]
Paralomis formosa	0.23	23	3	Forward	[103–105]
Kamchatka crab	8	150	3[a]	Forward	[105, 106]
Red king crab	10.9	152	0.1	Forward	[107, 116]
Coconut crab	37.3	123	50	Forward	[108, 117]
Our robot	3.65	29	7	Sideways	This paper
Our robot	3.65	29	4	Forward	This paper

[a]The average velocity is used. Maximum velocities are used for others. Note that these speeds are from a variety of sources from laboratory [110, 113] tests to migrations [103, 107], and are only provided to demonstrate the impressive range of animal scales.

shown in figure 8, are small and comparable, the slip of the other legs can be greater, figure 8. In particular in forward walking, the impacts of the alternating tripods are asymmetric at the onset of stance due to the fact that two feet fall on one side and one on the other side. Two legs on the right $(+Y)$ land at the same time as the middle leg on the left $(-Y)$, causing a COM displacement to the left (−Y), which will be corrected in the next alternating tripod [118–120]. While these offsets are small relative to the body width of the robot, as shown in figure C1 in appendix C, they can introduce wasted yaw rotation that is not present in sideways walking [121]. Both yaw rotation and slippage from front and rear legs, figure 8, result in smaller velocity of forward walking, which is visible in figure C1, and evident in lower energy efficiency. One reason that the decrease in energy efficiency from tile to sand is smaller for forward walking might be that the sand damps this oscillation. Compliance in the leg may be an important factor to consider in future.

8.3. Limitations and future work

A limitation of this study is that because a complete optimization of leg morphology and gait control was not performed, we cannot rule out the possibility that there could exist a faster forward gait, especially for the sand. Our approach has the advantage that the robot motions are constrained to be slow enough to be precise, which means that they could be adjusted for precise foot placement. If this constraint was lifted, and more variable path parameterization was used, a more complete and detailed optimization would be possible. However, such an optimization seems unlikely to double the speed of forward walking. If such an optimization was performed either *a priori* or during walking, the approach presented here provides a heuristic for an appropriate baseline.

Furthermore, our results could be sensitive to leg design. Our robot segment lengths were chosen based on a goal to grasp rocky terrain by taking advantage of valleys between spheres [122], it may be that optimizing the legs for forward walking will yield improved forward walking gaits. This may be an area in which the study of biological crabs will be relevant, especially since our calculated optimal corresponds to the leg ratio which is also found in sideways walking crabs [122]. Actuators inspired by artificial muscles may be able to provide different behaviors.

Even more, the end effector design can be a factor. Simpler end effectors might not be able to take advantage of the sideways rolling motion of the dactyls. Compliant end effectors can recover and store impact energy. End effectors with variable friction or attachment properties could be exploited to a greater degree with more adaptive control. Sensing could enable closed-loop slip reduction gaits.

Interesting future work would be to compare studies of different number of legs [123–133] or different leg configurations. For example, some robots are configured for agile omnidirectional walking [53–55], and may have spectrum of gaits that includes forward and sideways walking, unlike here in which sideways and forward walking represent qualitatively different behaviors.

While we hope this study encourages use of sideways walking gaits in future robots, we recognize that there are disadvantages for sideways walking. Having legs on the “sides” as in forward walking (rather than the front and back for sideways walking) means that sensors are not occluded by the legs. For example, mounting cameras and range finders on the front of the robot can enable careful footfall planning for forward waking. However, in surf zone, sand and water, vision may be less helpful than tactile exploration, which can explain why crabs but not insects use sideways walking. Another advantage of forward walking is that legs can be specialized for a forward motion [134], unlike for crabs which typically walk equally well left and right. An insect might use rear legs for power and forward legs for manipulation and a lobster can balance front claws and rear pleon. However, in robot design, having multiple redundant parallel legs with the same design can be robust and cost-effective.

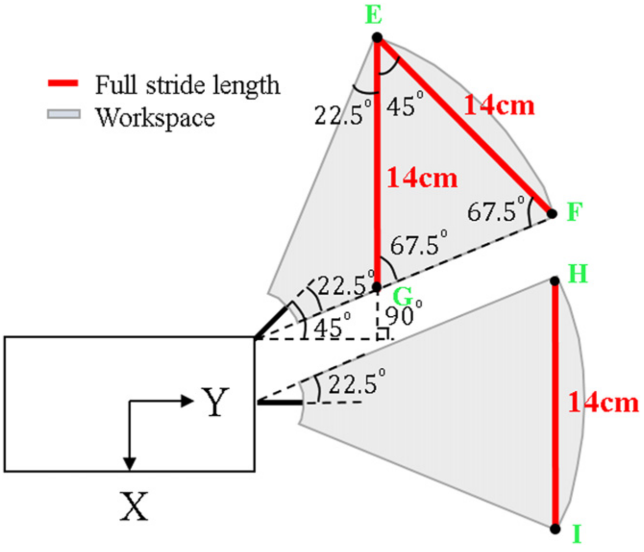

Figure A1. From the isosceles triangle defined in red, it can be shown that the front and rear legs' maximum SLs are equal to the middle leg's.

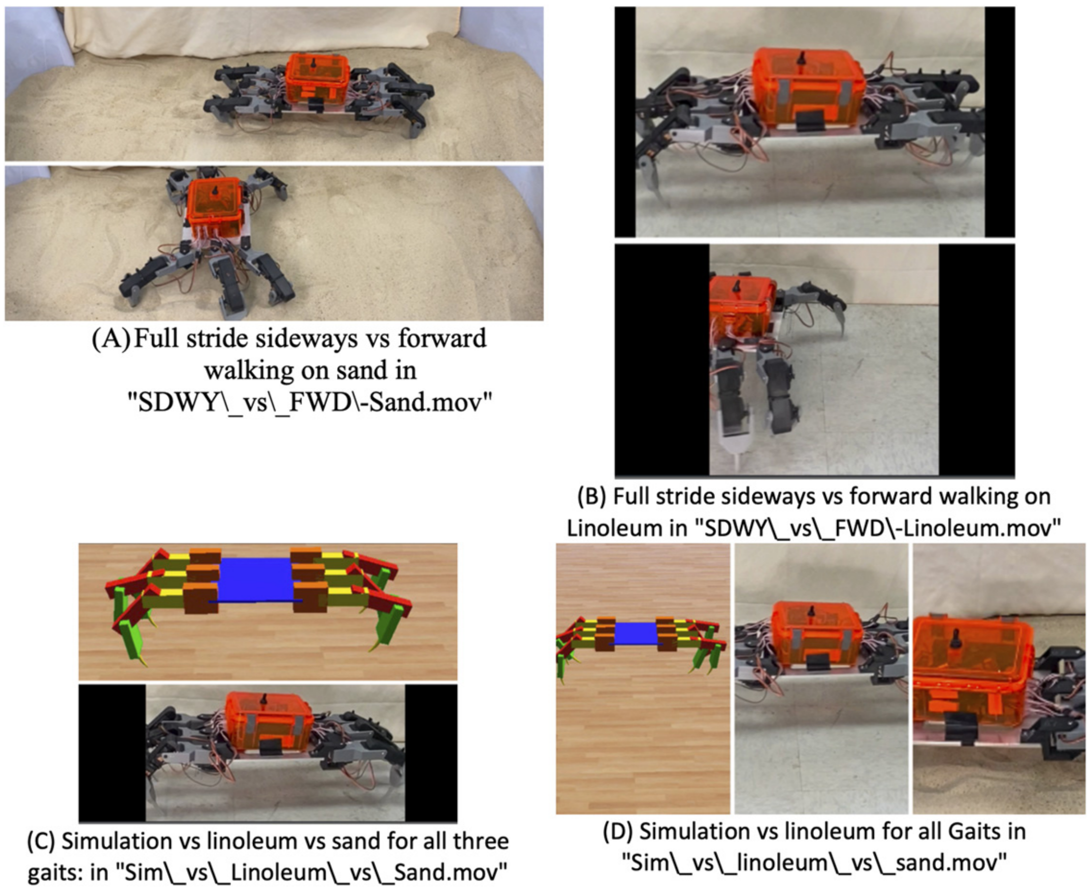

Figure B1. The overview of the main videos provided in the link.

Acknowledgments

The authors would like to acknowledge the anonymous reviewers whose valuable comments have improved this paper. This research was partially funded by the Office of Naval Research under a Young Investigator Award (TTP19-0033) and by the Strategic Environmental Research and Development Program (SERDP) SEED Grant #MR19-1369. The authors would like to thank Joseph Richmond for preliminary design, Yifeng Gong for the improvement of Sebastian robot, Nathan Carmichael for some figures and paper review, and Chunchu Zhu for the simulation suggestions. The authors would like to acknowl-

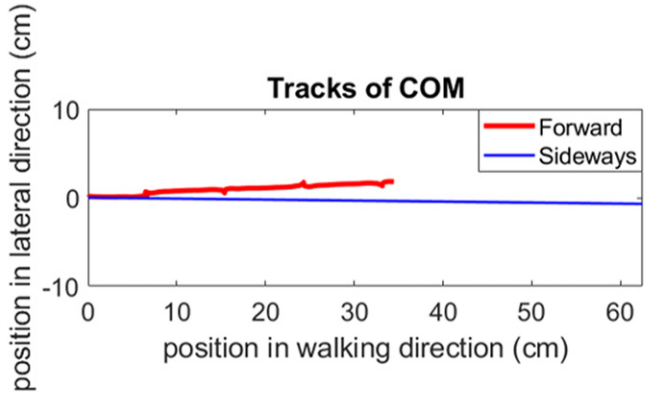

Figure C1. The blue and red lines show the tracks of COM for full stride sideways and forward walking within two cycles from simulation separately.

edge the anonymous reviewers whose valuable comments have improved this paper.

Data availability statement

The data that support the findings of this study are openly available at the following URL/DOI: https://drive.google.com/drive/folders/177CMmGKD1x23WKgBmd5N7fL3iEMmehJE.

Appendix A. The full stride lengths for front, rear and middle legs are the same

See Figure A1.

Appendix B. The videos of Webots dynamic simulation and Sebastian walking on linoleum floor and sand for all three gaits—full stride sideways and forward walking, and half stride sideways walking

See (Figure B1).

Appendix C. The tracks of the center of mass of Sebastian within two cycles

See Figure C1.

ORCID iDs

Yang Chen https://orcid.org/0000-0001-7380-5756
Nicole M Graf https://orcid.org/0000-0001-9207-0441

References

[1] Alexander R M 2013 *Principles of Animal Locomotion* (Princeton, NJ: Princeton University Press)
[2] Holmes P, Full R J, Koditschek D and Guckenheimer J 2006 The dynamics of legged locomotion: models, analyses, and challenges *SIAM Rev.* **48** 207–304
[3] Full R J 2000 Unlocking the secrets of animal locomotion Retrieve from https://berkeley.edu/news/media/releases/2002/09/rfull/robots.html
[4] Kinugasa T and Sugimoto Y 2017 Dynamically and biologically inspired legged locomotion: a review *J. Robot. Mechatron.* **29** 456–70
[5] Raibert M, Blankespoor K, Nelson G and Playter R 2008 BigDog, the rough-terrain quadruped robot *IFAC Proc. Vol.* **41** 10822–5
[6] Wooden D, Malchano M, Blankespoor K, Howardy A, Rizzi A A and Raibert M 2010 Autonomous navigation for BigDog *2010 IEEE Int. Conf. Robotics and Automation* (IEEE) pp 4736–41
[7] Boston Dynamics 2008 Mini, BDI Spot Retrieve from http://bostondynamics.com
[8] Michael K 2012 Meet Boston dynamics' LS3-the latest robotic war machine *Fac. Eng. Inf. Sci.* A 2773 https://ro.uow.edu.au/cgi/viewcontent.cgi?article=3782context=eispapers
[9] Hwangbo J, Lee J, Dosovitskiy A, Bellicoso D, Tsounis V, Koltun V and Hutter M 2019 Learning agile and dynamic motor skills for legged robots *Sci. Robot.* **4** eaau5872
[10] Darling K 2017 *'Who's Johnny?' Anthropomorphic framing in human-robot interaction, integration, and policy* Robot Ethics 2.0 ed P Lin, G Bekey, K Abney and R Jenkins (Oxford: Oxford University Press)
[11] Seok S, Wang A, Chuah M Y, Otten D, Lang J and Kim S 2013 Design principles for highly efficient quadrupeds and implementation on the MIT Cheetah robot *2013 IEEE Int. Conf. Robotics and Automation* (IEEE) pp 3307–12
[12] Daltorio K A, Horchler A D, Gorb S, Ritzmann R E and Quinn R D 2005 A small wall-walking robot with compliant, adhesive feet *2005 IEEE/RSJ Int. Conf. Intelligent Robots and Systems* (IEEE) pp 3648–53
[13] Daltorio K A *et al* 2008 A body joint improves vertical to horizontal transitions of a wall-climbing robot *2008 IEEE Int. Conf. Robotics and Automation* (IEEE) pp 3046–51
[14] Bender J A, Simpson E M, Tietz B R, Daltorio K A, Quinn R D and Ritzmann R E 2011 Kinematic and behavioral evidence for a distinction between trotting and ambling gaits in the cockroach *Blaberus discoidalis J. Exp. Biol.* **214** 2057–64
[15] Bjelonic M, Kottege N, Homberger T, Borges P, Beckerle P and Chli M 2018 Weaver: hexapod robot for autonomous navigation on unstructured terrain *J. Field Robot.* **35** 1063–79
[16] Roditis I, Nitsos T, Porichis A, Chatzakos P, Bertos G, Lika K and Papadopoulos E 2016 Maintaining static stability and continuous motion in rough terrain hexapod locomotion without terrain mapping *2016 24th Mediterranean Conf. Control and Automation (MED)* (IEEE) pp 545–50

[17] Spagna J C, Goldman D I, Lin P-C, Koditschek D E and Full R J 2007 Distributed mechanical feedback in arthropods and robots simplifies control of rapid running on challenging terrain *Bioinsp. Biomim.* **2** 9

[18] Sartoretti G, Shaw S, Lam K, Fan N, Travers M and Choset H 2018 Central pattern generator with inertial feedback for stable locomotion and climbing in unstructured terrain *2018 IEEE Int. Conf. Robotics and Automation (ICRA)* (IEEE) pp 5769–75

[19] Kim J-Y and Jun B-H 2014 Design of six-legged walking robot, little Crabster for underwater walking and operation *Adv. Robot.* **28** 77–89

[20] Kim B, Park S W, Lee P M and Jun B H 2011 Design of communication and video system for a multi-legged subsea robot *OCEANS 2011 IEEE-Spain* (IEEE) pp 1–6

[21] Kim B, Shim H, Yoo S Y, Lee G M, Jun B H and Lee P M 2013 Control architecture for stable gait of a six-legged subsea robot CR200 *2013 OCEANS-San Diego* (IEEE) pp 1–4

[22] Falconer J 2013 Huge six-legged robot Crabster goes swimming Retrieve from https://spectrum.ieee.org/six-legged-underwater-robot-crabster

[23] The Awesomer 2022 Robot spy crab Retrieve from https://theawesomer.com/robot-spy-crab/654219/

[24] Ishida M, Drotman D, Shih B, Hermes M, Luhar M and Tolley M T 2019 Morphing structure for changing hydrodynamic characteristics of a soft underwater walking robot *IEEE Robot. Autom. Lett.* **4** 4163–9

[25] Zhang J, Liu Q, Zhou J and Song A 2021 Crab-inspired compliant leg design method for adaptive locomotion of a multi-legged robot *Bioinsp. Biomim.* **17** 025001

[26] Ayers J, Witting J, Wilbur C, Zavracky P, McGruer N and Massa D 2000 Biomimetic robots for shallow water mine countermeasures *Proc. Autonomous Vehicles in Mine Countermeasures Symp.* vol 200

[27] Beer R D, Quinn R D, Chiel H J and Ritzmann R E 1997 Biologically inspired approaches to robotics: what can we learn from insects? *Commun. ACM* **40** 30–8

[28] Ijspeert A J 2008 Central pattern generators for locomotion control in animals and robots: a review *Neural Netw.* **21** 642–53

[29] Kim S and Wensing P M 2017 Design of dynamic legged robots *Found. Trends Robot.* **5** 117–90

[30] Graf N M, Behr A M and Daltorio K A 2019 Crab-like hexapod feet for amphibious walking in sand and waves *Conf. Biomimetic and Biohybrid Systems* (Springer) pp 158–70

[31] Graf N M, Behr A M and Daltorio K A 2021 Dactyls and inward gripping stance for amphibious crab-like robots on sand *Bioinsp. Biomim.* **16** 026021

[32] Sorin M O and Nițulescu M 2012 Hexapod robot leg dynamic simulation and experimental control using Matlab *IFAC Proc. Vol.* **45** 895–9

[33] Rojas M, Certad N, Cappelletto J and Grieco J C 2015 Foothold planning and gait generation for a hexapod robot traversing terrains with forbidden zones *2015 12th Latin American Robotics Symp. and 2015 3rd Brazilian Symp. Robotics (LARS-SBR)* (IEEE) pp 49–54

[34] Zha F, Chen C, Guo W, Zheng P and Shi J 2019 A free gait controller designed for a heavy load hexapod robot *Adv. Mech. Eng.* **11** 1687814019838369

[35] Rushworth A, Cobos-Guzman S, Axinte D and Raffles M 2015 Pre-gait analysis using optimal parameters for a walking machine tool based on a free-leg hexapod structure *Robot. Auton. Syst.* **70** 36–51

[36] Molnar T, Steindl R, Kottege N, Talbot F and Elfes A 2017 Steep terrain ascension controller for hexapod robots *Proc. Australasian Conf. Robotics and Automation*

[37] Coelho J, Ribeiro F, Dias B, Lopes G and Flores P 2021 Trends in the control of hexapod robots: a survey *Robotics* **10** 100

[38] Isvara Y, Rachmatullah S, Mutijarsa K, Prabakti D E and Pragitatama W 2014 Terrain adaptation gait algorithm in a hexapod walking robot *2014 13th Int. Conf. Control Automation Robotics and Vision (ICARCV)* (IEEE) pp 1735–9

[39] Tanaka G, Takamura T, Shimura Y, Motegi K and Shiraishi Y 2019 Development of simulator and analysis of walking for hexapod robots *2019 58th Annual Conf. Society of Instrument and Control Engineers of Japan (SICE)* (IEEE) pp 1594–9

[40] Khudher D, Powell R and Abbod M 2017 Operational space control in hexapod robot for humanitarian demining applications *2017 3rd Int. Conf. Control, Automation and Robotics (ICCAR)* (IEEE) pp 212–6

[41] Yu H, Gao H, Ding L, Li M, Deng Z and Liu G 2016 Gait generation with smooth transition using cpg-based locomotion control for hexapod walking robot *IEEE Trans. Ind. Electron.* **63** 5488–500

[42] Lewis M A, Fagg A H and Bekey G A 1993 Genetic algorithms for gait synthesis in a hexapod robot *Recent Trends in Mobile Robots* (Singapore: World Scientific) pp 317–31

[43] Schilling M, Paskarbeit J, Hoinville T, Hüffmeier A, Schneider A, Schmitz J and Cruse H 2013 A hexapod walker using a heterarchical architecture for action selection *Front. Comput. Neurosci.* **7** 126

[44] Lele A S, Fang Y, Ting J and Raychowdhury A 2020 Learning to walk: spike based reinforcement learning for hexapod robot central pattern generation *2020 2nd IEEE Int. Conf. Artificial Intelligence Circuits and Systems (AICAS)* (IEEE) pp 208–12

[45] Liu C, Li Z, Zhang C, Yan Y and Zhang R 2019 Gait planning and control for a hexapod robot on uneven terrain based on Markov decision process *2019 14th IEEE Conf. Industrial Electronics and Applications (ICIEA)* (IEEE) pp 583–6

[46] Heppner G, Roennau A, Oberländer J, Klemm S and Dillmann R 2015 LAUROPE-six legged walking robot for planetary exploration participating in the spacebot cup *Workshop Advanced Space Technologies for Robotics and Automation* vol 2 pp 69–76

[47] Deepa T, Angalaeswari S, Subbulekshmi D, Krithiga S, Sujeeth S and Kathiravan R 2021 Design and implementation of bio inspired hexapod for exploration applications *Mater. Today: Proc.* **37** 1603–7

[48] Buchanan R, Bandyopadhyay T, Bjelonic M, Wellhausen L, Hutter M and Kottege N 2019 Walking posture adaptation for legged robot navigation in confined spaces *IEEE Rob. Autom. Lett.* **4** 2148–55

[49] Yu J, Hooks J, Zhang X, Ahn M S and Hong D 2018 A proprioceptive, force-controlled, non-anthropomorphic biped for dynamic locomotion *2018 IEEE-RAS 18th Int. Conf. Humanoid Robots (Humanoids)* (IEEE) pp 1–9

[50] Yu J, Hooks J, Ghassemi S, Pogue A and Hong D 2016 Investigation of a non-anthropomorphic bipedal robot with stability, agility, and simplicity *2016 13th Int. Conf. Ubiquitous Robots and Ambient Intelligence (URAI)* (IEEE) pp 11–5

[51] Yu J, Hooks J, Ghassemi S and Hong D 2017 Exploration of turning strategies for an unconventional non-anthropomorphic bipedal robot *Int. Design Engineering Technical Conf. and Computers and Information in Engineering Conf.* vol 58189 (American Society of Mechanical Engineers) p V05BT08A021

[52] Hooks J, Ahn M S, Yu J, Zhang X, Zhu T, Chae H and Hong D 2020 ALPHRED: a multi-modal operations quadruped robot for package delivery applications *IEEE Rob. Autom. Lett.* **5** 5409–16

[53] Görner M, Wimböck T and Hirzinger G 2009 The DLR Crawler: evaluation of gaits and control of an actively compliant six-legged walking robot *Ind. Robot* **36** 344–51

[54] Irawan A and Nonami K 2012 Force threshold-based omni-directional movement for hexapod robot walking on

uneven terrain *2012 4th Int. Conf. Computational Intelligence, Modelling and Simulation* (IEEE) pp 127–32

[55] Estremera J, Cobano J A and Gonzalez de Santos P 2010 Continuous free-crab gaits for hexapod robots on a natural terrain with forbidden zones: an application to humanitarian demining *Robot. Auton. Syst.* **58** 700–11

[56] Mahapatra A, Roy S S and Pratihar D K 2019 Study on feet forces' distributions, energy consumption and dynamic stability measure of hexapod robot during crab walking *Appl. Math. Modelling* **65** 717–44

[57] Roy S S and Pratihar D K 2011 Dynamic modeling and energy consumption analysis of crab walking of a six-legged robot *2011 IEEE Conf. Technologies for Practical Robot Applications* (IEEE) pp 82–7

[58] Wang G, Chen X, Yang S, Jia P, Yan X and Xie J 2017 Subsea crab bounding gait of leg-paddle hybrid driven shoal crablike robot *Mechatronics* **48** 1–11

[59] All About Circuits 2017 The Crabster—a giant robotic crab that can do specific task Retrieve from https://youtube.com/watch?v=MnvemTwgYhw

[60] Discovery Canada 2016 Deep water Crabster Retrieve from https://youtube.com/watch?v=Ma80Ox2NLH0

[61] Lakatos D, Ploeger K, Loeffl F, Seidel D, Schmidt F, Gumpert T, John F, Bertram T and Albu-Schäffer A 2018 Dynamic locomotion gaits of a compliantly actuated quadruped with slip-like articulated legs embodied in the mechanical design *IEEE Rob. Autom. Lett.* **3** 3908–15

[62] Rönnau A, Heppner G, Nowicki M and Dillmann R 2014 LAURON V: a versatile six-legged walking robot with advanced maneuverability *2014 IEEE/ASME Int. Conf. Advanced Intelligent Mechatronics* (IEEE) pp 82–7

[63] Martinez M M 2001 Running in the surf: hydrodynamics of the shore crab *Grapsus tenuicrustatus J. Exp. Biol.* **204** 3097–112

[64] Blake R W 1985 Crab carapace hydrodynamics *J. Zool.* **207** 407–23

[65] Tsang L M, Chan T-Y, Ahyong S T and Chu K H 2011 Hermit to king, or hermit to all: multiple transitions to crab-like forms from hermit crab ancestors *Syst. Biol.* **60** 616–29

[66] Vidal-Gadea A G, Rinehart M D and Belanger J H 2008 Skeletal adaptations for forwards and sideways walking in three species of decapod crustaceans *Arthropod Struct. Dev.* **37** 95–108

[67] Michel O 2004 Cyberbotics Ltd. Webots$^{\text{TM}}$: professional mobile robot simulation *Int. J. Adv. Robot. Syst.* **1** 5

[68] Michel O 1998 Webots: symbiosis between virtual and real mobile robots *Int. Conf. Virtual Worlds* (Springer) pp 254–63

[69] Hohl L, Tellez R, Michel O and Ijspeert A J 2006 Aibo and Webots: simulation, wireless remote control and controller transfer *Robot. Auton. Syst.* **54** 472–85

[70] Pacheco J and Benito F 2005 Development of a Webots simulator for the Lauron IV robot *CCIA* pp 347–54

[71] Anam K, Effendi R, Santoso A and Jazidie A 2012 Autonomous five legs rescue robot navigation in cluttered environment *Acad. Res. Int. SAVAP* **2**

[72] Jiang M, Huang Z, Jiang G, Shi M and Zeng X 2017 Motion generation of multi-legged robot in complex terrains by using estimation of distribution algorithm *2017 IEEE Symp. Series on Computational Intelligence (SSCI)* (IEEE) pp 1–6

[73] Xin Y, Rong X, Li Y, Li B and Chai H 2019 Movements and balance control of a wheel-leg robot based on uncertainty and disturbance estimation method *IEEE Access* **7** 133265–73

[74] Liu C, Chen Y, Zhang J and Chen Q 2009 CPG driven locomotion control of quadruped robot *2009 IEEE Int. Conf. Systems, Man and Cybernetics* (IEEE) pp 2368–73

[75] Knüsel J, Crespi A, Cabelguen J, Ijspeert A J and Ryczko D 2020 Reproducing five motor behaviors in a salamander robot with virtual muscles and a distributed CPG controller regulated by drive signals and proprioceptive feedback *Front. Neurorob.* **14** 604426

[76] Ramdya P, Thandiackal R, Cherney R, Asselborn T, Benton R, Ijspeert A J and Floreano D 2017 Climbing favours the tripod gait over alternative faster insect gaits *Nat. Commun.* **8** 14494

[77] Grezmak J, Graf N, Behr A and Daltorio K 2021 Terrain classification based on sensed leg compliance for amphibious crab robot *IEEE Sens. J.*

[78] McMillan S 1994 Computational dynamics for robotic systems on land and under water *PhD Thesis* The Ohio State University

[79] Nishi J 1998 Gait pattern and energetic cost in hexapods *Proc. 20th Annual Int. Conf. IEEE Engineering in Medicine and Biology Society. Vol. 20 Biomedical Engineering Towards the Year 2000 and Beyond (Cat. No. 98CH36286)* vol 5 (IEEE) pp 2430–3

[80] Nishii J 2000 Legged insects select the optimal locomotor pattern based on the energetic cost *Biol. Cybern.* **83** 435–42

[81] Basu C K, Deacon F, Hutchinson J R and Wilson A M 2019 The running kinematics of free-roaming giraffes, measured using a low cost unmanned aerial vehicle (UAV) *PeerJ* **7** e6312

[82] Chen G, Jin B and Chen Y 2017 Tripod gait-based turning gait of a six-legged walking robot *J. Mech. Sci. Technol.* **31** 1401–11

[83] Lee T-T, Liao C-M and Chen T K 1988 On the stability properties of hexapod tripod gait *IEEE J. Robot. Autom.* **4** 427–34

[84] Barrio R, Lozano Á, Martínez M A, Rodríguez M and Serrano S 2021 Routes to tripod gait movement in hexapods *Neurocomputing* **461** 679–95

[85] Priandana K, Buono A and Wulandari 2017 Hexapod leg coordination using simple geometrical tripod-gait and inverse kinematics approach *2017 Int. Conf. Advanced Computer Science and Information Systems (ICACSIS)* (IEEE) pp 35–40

[86] Xu X Y, Yan G Z and Ding G Q 2002 Research on miniature hexapod bio-robot and its tripod gait [j] *Opt Precis. Eng.* **4** 392–6

[87] Nguyen C T, Phung H, Nguyen T D, Jung H and Choi H R 2017 Multiple-degrees-of-freedom dielectric elastomer actuators for soft printable hexapod robot *Sensors Actuators* A **267** 505–16

[88] Ritzmann R E, Quinn R D and Fischer M S 2004 Convergent evolution and locomotion through complex terrain by insects, vertebrates and robots *Arthropod Struct. Dev.* **33** 361–79

[89] Grzelczyk D, Stanczyk B and Awrejcewicz J 2017 Kinematics, dynamics and power consumption analysis of the hexapod robot during walking with tripod gait *Int. J. Struct. Stabil. Dynam.* **17** 1740010

[90] Liu Y, Fan X, Ding L, Wang J, Liu T and Gao H 2020 Fault-tolerant tripod gait planning and verification of a hexapod robot *Appl. Sci.* **10** 2959

[91] Marhefka D W and Orin D E 1997 Gait planning for energy efficiency in walking machines *Proc. Int. Conf. Robotics and Automation* vol 1 (IEEE) pp 474–80

[92] Nishii J, Ogawa K and Suzuki R 1998 The optimal gait pattern in hexapods based on energetic efficiency *Proc. 3rd Int. Symp. Artificial Life and Robotics* (Citeseer) pp 106–9

[93] Mahapatra A, Roy S S and Pratihar D K 2020 Optimal feet-forces' and torque distributions of six-legged robot maneuvering on various terrains *Robotica* **38** 1041–63

[94] Marhefka D W and Orin D E 1998 Quadratic optimization of force distribution in walking machines *Proc. 1998 IEEE Int. Conf. Robotics and Automation (Cat. No. 98CH36146)* vol 1 (IEEE) pp 477–83

[95] Wollherr D, Hardt M, Buss M and Von Stryk O 2002 Actuator selection and hardware realization of a small and fast-moving, autonomous humanoid robot *IEEE/RSJ Int. Conf. Intelligent Robots and Systems* vol 3 (IEEE) pp 2491–6

[96] Jin B, Chen C and Li W 2013 Power consumption optimization for a hexapod walking robot *J. Intell. Robot. Syst.* **71** 195–209

[97] Ishiguro A, Kawasumi K and Fujii A 2002 Increasing evolvability of a locomotion controller using a passive-dynamic-walking embodiment *IEEE/RSJ Int. Conf. Intelligent Robots and Systems* vol 3 (IEEE) pp 2581–6

[98] Endo K, Maeno T and Kitano H 2003 Co-evolution of morphology and walking pattern of biped humanoid robot using evolutionary computation: designing the real robot *2003 IEEE Int. Conf. Robotics and Automation (Cat. No. 03CH37422)* vol 1 (IEEE) pp 1362–7

[99] Silva M F and Machado J T 2012 A literature review on the optimization of legged robots *J. Vib. Control* **18** 1753–67

[100] Doppelhammer N, Baumgartner W and Vereshchaga Y 2018 Interplay between stride velocity, stride frequency and stride length in human gait transition *J. Bioanal. Biomed.* **10** 74–9

[101] Prágr M, Čížek P and Faigl J 2018 Cost of transport estimation for legged robot based on terrain features inference from aerial scan *2018 IEEE/RSJ Int. Conf. Intelligent Robots and Systems (IROS)* (IEEE) pp 1745–50

[102] Watson-Zink V M 2021 Making the grade: physiological adaptations to terrestrial environments in decapod crabs *Arthropod Struct. Dev.* **64** 101089

[103] Collins M, Yau C, Guilfoyle F, Bagley P, Everson I, Priede I G and Agnew D 2002 Assessment of stone crab (*Lithodidae*) density on the south Georgia slope using baited video cameras *ICES J. Mar. Sci.* **59** 370–9

[104] Morley S A, Belchier M, Dickson J and Mulvey T 2006 Reproductive strategies of sub-Antarctic lithodid crabs vary with habitat depth *Polar Biol.* **29** 581–4

[105] Ocean Explorer 2003 Adaptations of crabs to life in the deep sea Retrieve from https://oceanexplorer.noaa.gov/explorations/02alaska/background/crabs/crabs.html

[106] X-Ray Mag 2003 Invasion of the king crabs Retrieve from https://xray-mag.com/content/invasion-king-crabs

[107] Jørgensen T, Løkkeborg S, Anders F and Hufthammer M 2007 Walking speed and area utilization of red king crab (*Paralithodes camtschaticus*) introduced to the Barents Sea coastal ecosystem *Developments in Fish Telemetry* (Berlin: Springer) pp 17–24

[108] Weird Nature 2021 13 facts most people don't know about the coconut crab, the biggest arthropod Retrieve from https://ranker.com/list/scary-coconut-crab-facts/jen-jeffers

[109] Burrows M and Hoyle G 1973 The mechanism of rapid running in the ghost crab, *Ocypode ceratophthalma J. Exp. Biol.* **58** 327–49

[110] Hui C A 1992 Walking of the shore crab *Pachygrapsus crassipes* in its two natural environments *J. Exp. Biol.* **165** 213–27

[111] Gross W J and Marshall L A 1960 The influence of salinity on the magnesium and water fluxes of a crab *Biol. Bull.* **119** 440–53

[112] Wikipedia 2021 *Pachygrapsus crassipes* Retrieve from https://en.wikipedia.org/wiki/Pachygrapsus_crassipes

[113] Blickhan R and Full R J 1987 Locomotion energetics of the ghost crab: II. Mechanics of the centre of mass during walking and running *J. Exp. Biol.* **130** 155–74

[114] Animal Spot 2022 Ghost crab (sand crab) Retrieve from https://animalspot.net/ghost-crab-sand-crab.html#Length

[115] Animal Diversity Web 2022 *Ocypode quadrata* Atlantic ghost crab Retrieve from https://animaldiversity.org/accounts/Ocypode_quadrata/

[116] NOAA fisheries 2022 Red king crab Retrieve from https://fisheries.noaa.gov/species/red-king-crab

[117] Animal Picture Archive 2021 How fast can a coconut crab run? Retrieve from https://animalpicturesarchive.com/how-fast-can-a-coconut-crab-run/

[118] Schmitt J and Holmes P 2000 Mechanical models for insect locomotion: dynamics and stability in the horizontal plane i. theory *Biol. Cybern.* **83** 501–15

[119] Schmitt J and Holmes P 2000 Mechanical models for insect locomotion: dynamics and stability in the horizontal plane: II. Application *Biol. Cybern.* **83** 517–27

[120] Full R J, Kubow T, Schmitt J, Holmes P and Koditschek D 2002 Quantifying dynamic stability and maneuverability in legged locomotion *Integr. Comp. Biol.* **42** 149–57

[121] Martinez M, Full R and Koehl M 1998 Underwater punting by an intertidal crab: a novel gait revealed by the kinematics of pedestrian locomotion in air versus water *J. Exp. Biol.* **201** 2609–23

[122] Chen Y, Clifton G, Graf N M, Durand K, Taylor J and Daltorio K 2022 Optimal geometry for planar robotic limbs stepping over obstacles parallels that found in crabs *Bioinsp. Biomim.* (submitted)

[123] Fankhauser P and Hutter M 2018 ANYmal: a unique quadruped robot conquering harsh environments *Res. Features* **126** 54–7

[124] Lee J, Hwangbo J, Wellhausen L, Koltun V and Hutter M 2020 Learning quadrupedal locomotion over challenging terrain *Sci. Robot.* **5** eabc5986

[125] Liu Y, Bi Q and Li Y 2021 Design of a bio-inspired quadruped robot with scalable torso *2021 IEEE 17th Int. Conf. Automation Science and Engineering (CASE)* (IEEE) pp 455–60

[126] Shi F, Homberger T, Lee J, Miki T, Zhao M, Farshidian F, Okada K, Inaba M and Hutter M 2021 Circus ANYmal: a quadruped learning dexterous manipulation with its limbs *2021 IEEE Int. Conf. Robotics and Automation (ICRA)* (IEEE) pp 2316–23

[127] Biswal P and Mohanty P K 2021 Development of quadruped walking robots: a review *Ain Shams Eng. J.* **12** 2017–31

[128] Katz B, Carlo J D and Kim S 2019 Mini Cheetah: a platform for pushing the limits of dynamic quadruped control *2019 Int. Conf. Robotics and Automation (ICRA)* pp 6295–301

[129] Park H-W, Wensing P M and Kim. S 2021 Jumping over obstacles with MIT Cheetah 2 *Robot. Auton. Syst.* **136** 103703

[130] Vidoni R and Gasparetto A 2011 Efficient force distribution and leg posture for a bio-inspired spider robot *Robot. Auton. Syst.* **59** 142–50

[131] Robugtix T8x 2022 Retrieve from https://robugtix.com/t8x

[132] Neubauer W 1994 A spider-like robot that climbs vertically in ducts or pipes *Proc. of IEEE/RSJ Int. Conf. Intelligent Robots and Systems (IROS'94)* vol 2 (IEEE) pp 1178–85

[133] Zhong G, Chen L and Deng H 2017 A performance oriented novel design of hexapod robots *IEEE/ASME Trans. Mechatronics* **22** 1435–43

[134] Graham D 1972 A behavioural analysis of the temporal organisation of walking movements in the 1st instar and adult stick insect (*Carausius morosus*) *J. Comp. Physiol.* **81** 23–52